

Figure 4 The GluN2 S/L site contributes to NMDAR subtype specificity of relative Ca^{2+} permeability. **(a,b)** Representative I - V curves in 143 mM extracellular Cs^+ **(a)** and 1.8 mM extracellular Ca^{2+} **(b)**. **(c,d)** Average $V_{\text{rev}} \pm$ s.e.m. of wild-type and mutant NMDARs in 143 mM extracellular Cs^+ **(c)** and 1.8 mM extracellular Ca^{2+} **(d)**. No significant differences were detected among wild-type and mutant receptor V_{rev} in 143 mM extracellular Cs^+ (one-way ANOVA, $P = 0.45$). Significantly different V_{rev} values (one-way ANOVA followed by Tukey *post hoc* comparison, $P < 0.05$) between wild-type and mutant receptors are marked with an asterisk. **(e)** $P_{\text{Ca}}/P_{\text{Cs}}$ values of wild-type and mutant NMDARs.

GluN1/2A(S632L) receptors was 34.8 ± 1.4 pS, which was significantly different from the GluN1/2A receptor main state conductance (t test for heterogeneity of slopes, $P < 0.0001$), but not significantly different ($P = 0.25$) from that of GluN1/2D receptors (37.4 ± 1.3 pS, measured previously¹⁵ and consistent with other reported values²¹). The GluN1/2D(L657S) receptor main state conductance was 54.9 ± 1.5 pS, which was significantly different from the GluN1/2D receptor main state conductance¹⁵ ($P < 0.0001$), but not significantly different from that of GluN1/2A receptors ($P = 0.23$).

Another single-channel property that distinguishes NMDAR subtypes is the prominent subconductance state of ~ 20 pS that is exhibited by GluN1/2C and GluN1/2D receptors^{15,21}; in contrast, GluN1/2A or GluN1/2B receptors exhibit a larger subconductance state (~ 40 pS)²⁰ that is less commonly occupied. GluN1/2A(S632L) receptors exhibited a subconductance state with a conductance (17.0 ± 0.7 pS) that was not significantly different from the subconductance state of GluN1/2D receptors (20.2 ± 1.3 pS, $P = 0.052$; **Fig. 5c**). In contrast, the GluN1/2D(L657S) receptor subconductance state was 49.6 ± 5.6 pS, which was significantly higher than that of GluN1/2D receptors ($P < 0.0001$). We could not consistently resolve a subconductance state in GluN1/2A receptors, although a subconductance state of ~ 40 pS was occupied infrequently in some patches. Our ability to consistently resolve the subconductance state of GluN1/2D and GluN1/2D(L657S) receptors, but not of GluN1/2A receptors, suggests that subconductance state occupancy by GluN1/2D receptors was not markedly reduced by the mutation. Thus, mutation of the GluN2 S/L site in GluN2D receptors has a powerful effect on the

conductance of the subconductance state, but appears to have a weaker effect on subconductance state occupancy.

To determine whether single-channel kinetics are influenced by the GluN2 S/L site, we constructed open period and shut time histograms (**Supplementary Fig. 2** and **Supplementary Table 2**) and statistically compared the values of weighted mean open periods. The weighted mean open periods of GluN1/2A and GluN1/2A(S632L) receptors were not significantly different (one-way ANOVA followed by Tukey *post hoc* comparison, $P = 0.70$), nor were the weighted mean open periods of GluN1/2D and GluN1/2D(L657S) receptors ($P = 0.84$; see **Supplementary Table 2**). Thus, consistent with previous studies showing that NMDAR subtype-dependence of channel gating depends on the N-terminal domain^{8,9}, the GluN2 S/L site does not appear to have a substantial effect on channel kinetics.

We conclude that the naturally occurring residue replacement in GluN2 subunits that we mimicked by creating GluN2A(S632L), GluN2C(L643S) and GluN2D(L657S) subunits underlies fundamental NMDAR subtype-dependent variations in multiple channel characteristics: Mg^{2+} block, relative Ca^{2+} permeability, and single-channel conductance of both main and subconductance states. However, the way in which the GluN2 S/L site affects pore properties is unclear on the basis of the above data.

Mechanism of GluN2 S/L site influence on Mg^{2+} block

To search for the mechanisms by which the GluN2 S/L site transmits its effects to the pore, we created additional GluN2A subunits with mutations at the GluN2 S/L site and tested whether the Mg^{2+} IC_{50}

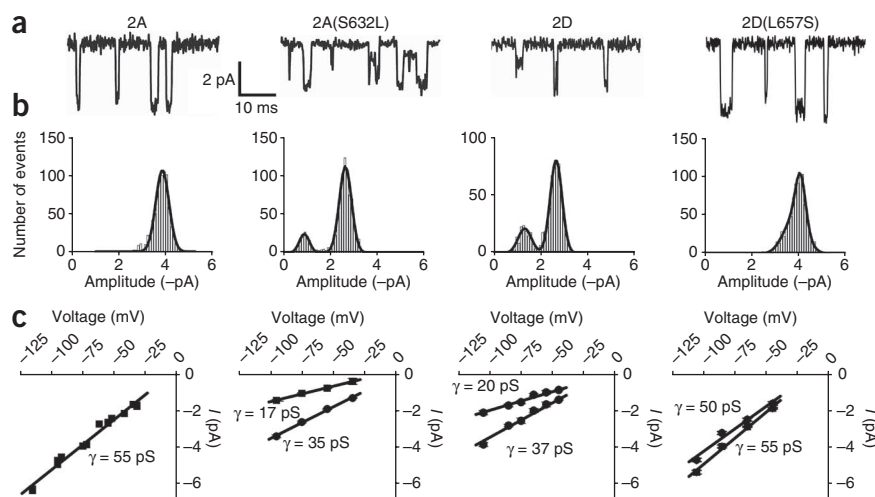


Figure 5 The GluN2 S/L site controls the NMDAR subtype specificity of single-channel conductance. **(a,b)** Representative single-channel current traces **(a)** and amplitude histograms **(b)** of GluN1/2A (left), GluN1/2A(S632L) (center left), GluN1/2D (center right) and GluN1/2D(L657S) (right) receptors recorded in the outside-out patch configuration at -75 mV. **(c)** Current versus voltage plots of single-channel currents and linear regression fits. The slope of the linear fit to each plot (single-channel conductance) is shown next to each fit. Left, GluN1/2A receptors ($n = 17$ single-channel current recordings); center left, GluN1/2A(S632L) receptors ($n = 17$); center right, GluN1/2D receptors ($n = 24$; GluN1/2D data from ref. 15); right, GluN1/2D(L657S) receptors ($n = 16$).